DURABILITY ANALYSIS AND IMPLEMENTATION OF THE FLOATING FRAME OF REFERENCE FORMULATION

Ahmed A. Shabana[1] (shabana@uic.edu
Gengxiang Wang[2] (gengxiangwang@gmail.com)

[1]Department of Mechanical and Industrial Engineering, University of Illinois at Chicago, 842 West Taylor Street, Chicago, Illinois 60607
[2]Faculty of Mechanical and Precision Instrument Engineering, Xi'an University of Technology, Xi'an 710048, Shaanxi, P.R. China

ABSTRACT

The finite element (FE) *floating frame of reference* (FFR) formulation, implemented in most commercial multibody system (MBS) computer programs, is widely used in the *durability analysis* by a large number of industry sectors. In this paper, a single-degree of freedom system is used to derive a new analytical model from the general nonlinear FFR equations. The obtained new analytical model is used to address fundamental issues related to the accurate, efficient, and general implementation of the FFR formulation, including the treatment of the algebraic joint constraint equations, fundamental difference between the FFR *reference conditions* and the structural mechanics *boundary conditions*, the choice of the deformation modes, handling redundant MBS constraints, effect of the MBS joints on the oscillation frequencies, and difference between fixed and moving boundary conditions. Structural mechanics boundary conditions eliminate degrees of freedom and define the system topology, while the FFR reference conditions eliminate coordinate redundancy and do not introduce any motion constraints. The paper shows analytically how the MBS joint constraint equations change the system oscillation frequencies, demonstrates the effect of using inappropriate set of reference conditions, proves there is no single set of reference conditions suited for all applications, and uses other FE methods to verify the results and support the conclusions drawn. The results obtained in this investigation show that improper selection of the reference conditions can lead to solution errors that exceed 100%, making such a solution completely unreliable in any durability investigation. General implementation of the FFR formulation will significantly contribute to increasing reliance on virtual testing, less reliance on building actual prototypes, better understanding of flexible body dynamics, and better communication between various computer-aided engineering (CAE) groups.

Keywords: Durability analysis; floating frame of reference formulation; reference conditions; boundary conditions; multibody system dynamics.

1. INTRODUCTION

Multibody system (MBS) formulations, computational algorithms, and software are widely used in the analysis of mechanical and aerospace systems (Hegazy et al, 1999; Ho, 1977; Ho and Herber, 1985; Hooker, 1975; Jerkovsky, 1978; Kane and Levinson, 1983; Kane and Levinson, 1985; Kushwaha et al, 2002; Likins, 1973; Liu et al, 2011; Magnus, 1978; Orlandea et al, 1977; Rahnejat, 2000; Roberson and Schwertassek, 1988; Schiehlen, 1982; Udwadia and Schutte, 2010; Udwadia and Wanichanon, 2010; Wittenburg, 1977). Accurate flexible body modeling, including accurate prediction of the large displacements, forces, and stresses under different loading conditions, is central in any credible durability investigation. In the CAE durability analysis, multibody system (MBS) computer programs are often used to analyze the deformations using the finite element (FE) *floating frame of reference* (FFR) formulation. While the FFR formulation was introduced more than a century ago, the FE/FFR formulation, which allows for modeling complex geometries, was introduced in the early eighties. Prior to introducing the FE/FFR formulation, the stresses were obtained using a two-step analysis. In the first step, the system is assumed to consist of rigid bodies, and rigid body analysis is performed to determine the inertia and constraint forces. In the second step, the forces, predicted using the rigid body analysis, are used in a linear FE problem to determine the component stresses. This approach, which is referred to in the literature as the *linear theory of elasto-dynamics*, is based on the assumption that the component deformation has no effect on its rigid body displacement, and therefore, the dynamic coupling between the rigid body and elastic displacements of the system components is neglected (Bahgat and Willmert, 1973; Chu and Pan, 1975; Erdman and Sandor, 1972; Lowen and Chassapis, 1986; Lowen, G.G., and Jandrasits, W.G., 1972; Sadler and Sandor, 1973; Sunada and Dubowsky, 1981; Sunada and Dubowsky, 1983; Turcic and Midha,

3

1984). Since the FE/FFR formulation was introduced, the sequence of computations was reversed, and FE computer programs are currently used as preprocessors for MBS computer programs, which were designed to solve the differential and algebraic equations of constrained systems that consist of interconnected rigid and deformable bodies. Nonetheless, the capabilities of flexible MBS computer programs are not fully exploited as evident by the fact that the durability analysis still heavily relies on a conventional FE analysis for each system component at a time rather than using flexible MBS algorithms that allow for the analysis of the assembled system by incorporating the effect of mechanical joints.

Despite the fact that the FE/FFR formulation is implemented in most commercial MBS computer programs, there are important implementation issues that need to be addressed in order to obtain more credible durability results and increase reliance on virtual testing grounds that can have significant economic impact. The use of conventional FE approach to determine component strength in durability investigations can be error-prone in the case of MBS applications, as will be discussed in this paper. Reliable virtual prototyping techniques will allow the CAE engineers to efficiently experiment with different design configurations that can be prohibitively expensive or even impossible to explore using actual testing. Nonetheless, MBS computer programs that allow for system assembly are still not the main tools used for the durability investigations by many industrial organizations. Instead, MBS computer programs are often used in a rigid body analysis to predict the overall kinematic motion and loads that are used as input in a conventional FE analysis with the aim of evaluating the component strength. This is in fact equivalent to the use of the linear theory of elasto-dynamics that has proven inaccurate when considering mechanical systems. As a result, not only the quality of the durability investigations has been compromised, but also the lack of understanding of fundamental issues has caused damage to the

4

collegial relationship between different CAE groups and has hindered more reliance on virtual prototyping and testing, causing significant economic loss, and significant waste of time, efforts, and resources that can be better used to improve the product quality.

The quality of the durability analysis can be significantly enhanced by having better understanding of the FE/FFR formulation implemented in most commercial MBS computer programs. In the automotive industry for example, the results of a conventional FE stress analysis of the vehicle flexible components (frame, leaf springs, rods, etc.) with boundary conditions that do not reflect the actual nonlinear MBS joints, road profiles, and motion trajectories of the assembled vehicle can be misleading, as will be discussed in this paper. Furthermore, as demonstrated in this paper, a frequency analysis, that does not take into account the MBS joint formulations, may not accurately reflect the actual frequencies of oscillations of the vehicle components under realistic operating conditions. Building bulky and stiff components by over-designing does not contribute to improving the product quality or reducing its cost. In order to obtain accurate MBS simulations of the assembled vehicle under different loading and operating conditions, however, it is necessary to have good understanding of FE/FFR implementation issues in order to avoid performing unnecessary and costly analysis often based on wrong assumptions.

2. FE/FFR IMPLEMENTATION AND DURABILITY ANALYSIS

It is the main objective of this paper to develop a new and simple analytical model whose results can be verified using commercial FE computer programs. The new analytical model derived using the general FE/FFR nonlinear equations, also summarized in this paper, will serve to obtain new results that shed light on serious problems encountered in the durability analysis.

5

This paper addresses the following important FE/FFR implementation issues using the new analytical model that can serve as a benchmark example:

1. Using the FFR *mean-axis reference conditions*, MBS *joint constraints*, and MBS *embedding technique*, the equations of motion of a structural system is systematically reduced to a single-degree of freedom analytical model which has a closed form solution that can be used to shed light on fundamental FFR implementation issues. The FFR mean-axis conditions are used to eliminate the coordinate redundancy and define a unique displacement field, the MBS joint constraints are used to define the system topology and degrees of freedom, and the embedding technique is used to systematically eliminate the dependent variables and obtain a reduced order model from which the algebraic constraint equations are eliminated.

2. The paper demonstrates the fundamental difference between the structural mechanics *boundary conditions* used in the classical vibration theory and conventional FE approaches and the *reference conditions* used in the MBS approach. The structural mechanics boundary conditions eliminate degrees of freedom, define the system topology, and define the frequency contents in the solution; while the FE/FFR reference conditions eliminate coordinate redundancy, define a unique displacement field, do not define the frequency contents in the MBS system solution, and do not define the system topology which is defined in the FFR formulation using the MBS joint constraints. As shown in this paper, some sets of MBS reference conditions do not have equivalent structural mechanics boundary conditions when some models are considered. The phrase "boundary conditions" is loosely used in the literature to refer to the "reference conditions", but in general the two sets of conditions are not equivalent. The fundamental differences between the structural mechanics boundary and FFR reference conditions and the *sub-structuring interface conditions* are also discussed.

6

3. The *generality* of the FE/FFR formulation can be severely limited by restricting the choice of the FFR *reference conditions* to one set. In general-purpose flexible MBS algorithms, the choice of the deformation basis vectors should not be limited to one set. Using the new analytical model, it is shown that such a restriction can lead to wrong solutions with very significant error, demonstrating that one set of reference conditions is not suited for all applications. The results obtained in this investigation show that improper selection of the reference conditions can lead to solution errors that exceed 100%, making such a solution completely unreliable for any credible durability investigation.

4. CAE groups in the industry often perform FE durability analysis using *FE boundary conditions*. This paper discusses this important and fundamental issue by demonstrating that MBS joints change the solution dynamics characteristics, and therefore, durability analysis must be performed in a MBS computational environment. The *oscillation frequencies* of a single component can be significantly different from the oscillation frequencies of the same component in the assembled model. The single-degree of freedom analytical model developed in this study will be used to demonstrate the significant differences between the oscillation frequencies of the linear FE problem and the problem in which the MBS joints are imposed. This single-degree of freedom analytical model will be used to demonstrate that the *resonance frequency* significantly changes as the result of imposing the MBS joints, even in the case of a linear model in which rigid body motion is not allowed.

5. In the FE/FFR formulation, there are *external forces* associated with the reference motion as well as external forces associated with the FE elastic nodal coordinates. The use of an FE model in the durability analysis that considers only the nodal forces associated with the FE degrees of freedom leads to a model that is not consistent with the basic analytical dynamics

7

principles. The simple analytical model considered in this study shows that if the forces associated with the reference (rigid body) coordinates are not properly projected when developing an FE model, such an FE model will lead to wrong solutions. The MBS *embedding technique* is used to demonstrate this important fact.

6. The analytical model is used to discuss the important problem of handling *redundant constraints* in computational MBS algorithms. In some scenarios, as demonstrated in this paper, automatic elimination of redundant constraints can lead to a different model that has dynamics characteristics that are significantly different from those of the original model. The paper discusses the difference between *topological singularities* and *initial-configuration singularities*. It is shown that constraint redundancy can be associated with a particular initial configuration, and therefore, automatic removal of the constraints may not be a proper solution to this problem.

The analysis presented in this paper also sheds light on the difference between the reference conditions used to define a unique displacement field and the MBS joint constraint equations used to define the system topology. The MBS joint constraints eliminate kinematic degrees of freedom and impose restrictions on the motion of the assembled system, while reference conditions do not impose such a restriction. Before imposing the MBS joint constraints, the displacement field of all bodies, rigid and flexible, must be uniquely defined. Figure 1 shows planar and spatial spherical pendulums. The MBS joint constraints for these two simple systems require that the joint definition point on the pendulum remains fixed. This condition leads to two equations for the planar pendulum and three equations for the spatial spherical pendulum. This number of constraint equations is not sufficient in the FE/FFR formulation to define a unique displacement field. Furthermore, these equations are introduced to eliminate two degrees of

freedom in the case of the planar model and three degrees of freedom in the case of the spatial model, and are not introduced for the purpose of defining a unique displacement field for one of the bodies connected by the joint. The reference conditions, on the other hand, should not eliminate any kinematic degrees of freedom since they are used for the purpose of correctly defining the body displacement field. Coordinate reductions should not also be viewed as kinematic constraints imposed on the overall motion of the system since coordinate reduction techniques are mainly used to eliminate modes of deformation which have no significant effect on the overall motion of the system. Throughout this paper, simple examples are used to discuss the concepts addressed in this investigation.

3. FFR FORMULATION AND REFERENCE CONDITIONS

In this section, a brief review of the basic nonlinear FE/FFR equations is presented. The presentation of these equations is necessary since they will be systematically reduced to obtain the analytical model used in this investigation. Reference will be made to these general equations in order to explain how they can be simplified to obtain the analytical model whose results are compared with the results obtained using a general-purpose MBS computer program that employs a solution algorithm based on the general nonlinear equations presented in this section.

In order to ensure the generality and accuracy of the FE/FFR formulation implementation, it is necessary to understand the basic concepts used in the development of this approach that allows for modeling structures with geometric discontinuities (Shabana, 2013). The FFR formulation introduced more than a century ago is only suited for the analysis of simple structures such as beams and plates with simple geometries. The geometric discontinuity can be solved using the FE/FFR concept of the *intermediate element coordinate system* introduced in

9

the early eighties; a concept that resembles the parallel axis theorem and allows for correctly accounting for the rigid body inertia of the flexible components. Another important FE/FFR concept that must be understood and will be one of the main topics discussed in this investigation is the *reference conditions* used to eliminate the FE shape function rigid body modes and define the shape of deformation with respect to the body coordinate system. As will be shown in this investigation, restricting the choice of the reference conditions can lead to an FE/FFR implementation that is far from being general and can also lead to wrong solutions even if very simple systems are considered. In the FFR formulation, the configuration of the body is defined using the kinematic equation $\mathbf{r} = \mathbf{r}_O + \mathbf{A}\bar{\mathbf{u}}$, where $\mathbf{r}$ is the position vector of an arbitrary point on the body defined in the global coordinate system, $\mathbf{r}_O$ is the global position vector of the origin of the body coordinate system, $\mathbf{A}$ is the orthogonal transformation matrix that defines the orientation of the body coordinate system, and $\bar{\mathbf{u}}$ is the local position vector of the arbitrary point with respect to the body coordinate system. Differentiating the preceding equation with respect to time, the absolute velocity vector of the arbitrary point on the body can be written as $\dot{\mathbf{r}} = \dot{\mathbf{r}}_O + \dot{\mathbf{A}}\bar{\mathbf{u}}$. The velocity vector can also be written in the alternate forms $\dot{\mathbf{r}} = \dot{\mathbf{r}}_O + \mathbf{A}(\bar{\boldsymbol{\omega}} \times \bar{\mathbf{u}})$ and $\dot{\mathbf{r}} = \dot{\mathbf{r}}_O + \boldsymbol{\omega} \times \mathbf{u}$, where $\boldsymbol{\omega}$ and $\bar{\boldsymbol{\omega}}$ are, respectively, the angular velocity vectors defined in the global and body coordinate systems.

3.1   FE Discretization

In the FE/FFR formulation, a body coordinate system $X_1^b X_2^b X_3^b$ that shares the large overall displacement of the body is introduced. The position vector of the origin of the body coordinate system is defined by the three-dimensional vector $\mathbf{r}_O$, while the orientation of the body-coordinate system is defined using the orthogonal transformation matrix $\mathbf{A}$. The unconstrained

motion of the coordinate system of the body can then be described using six independent

coordinates; three translational coordinates $\mathbf{r}_O = \begin{bmatrix} \mathbf{r}_{O1} & \mathbf{r}_{O2} & \mathbf{r}_{O3} \end{bmatrix}^{\mathrm{T}}$, and three independent rotation

parameters $\boldsymbol{\theta}$ that define the orthogonal matrix $\mathbf{A}$. Using these coordinates, the global position

vector of an arbitrary point on the finite element j of the body can be written as

$$\mathbf{r}^j = \mathbf{r}_O + \mathbf{A}\overline{\mathbf{u}}^j , \qquad j = 1, 2, \ldots, n_e \tag{1}$$

where n_e is the total number of elements used in the FE discretization, and $\overline{\mathbf{u}}^j$ is the location of

the arbitrary point on the element j with respect to the origin of the body coordinate system. In

the preceding equation, $\mathbf{r}_O$ and $\mathbf{A}$ are the same for all finite elements, and therefore, the body

coordinate system represents a common reference for all elements and serves as the basis for

defining the connectivity between the elements of the body. In the FE/FFR formulation, one can

write $\overline{\mathbf{u}}^j = \mathbf{S}_b^j \mathbf{e}^j$, $j = 1, 2, \ldots n_e$, where $\mathbf{S}_b^j$ is an appropriate element shape function that accounts

for the intermediate element coordinate system transformations, and $\mathbf{e}^j$ is the vector of the

element nodal coordinates defined in the body coordinate system (Shabana, 2013, Chapter 6).

This vector of element nodal coordinates defines the position of the arbitrary point in the

undeformed state as well as the deformation vector, with the assumption that the element shape

function can describe an arbitrary large translations, a condition satisfied by all elements. In this

case, the vector of the element nodal coordinates can be written as $\mathbf{e}^j = \mathbf{e}_o^j + \mathbf{e}_f^j$, where $\mathbf{e}_o^j$ is the

vector of nodal coordinates in the undeformed reference configuration, and $\mathbf{e}_f^j$ is the vector of

nodal deformations.

3.2 FE/FFR Dynamic Equations

Using the Boolean matrix approach, the element nodal coordinates can be written in terms of the

body nodal coordinates as $\mathbf{e}^j = \mathbf{B}_c^j \mathbf{e}_b$, $j = 1, 2, \ldots n_e$, where $\mathbf{e}_b$ is the vector of the body nodal

coordinates, and $\mathbf{B}_c^j$ is the constant Boolean matrix that defines the connectivity conditions for the finite element j. Therefore, the position vector of the material points can be defined as $\overline{\mathbf{u}}^j = \mathbf{S}_b^j \mathbf{B}_c^j \mathbf{e}_b$, $j = 1, 2, \ldots n_e$.

As in the case of the individual elements, one can write the vector of body nodal coordinates as the sum of two vectors as $\mathbf{e}_b = \mathbf{e}_{bo} + \mathbf{e}_{bf}$, where $\mathbf{e}_{bo}$ is the vector of nodal coordinates in the initial un-deformed configuration, and $\mathbf{e}_{bf}$ is the vector of deformation nodal coordinates. The reference conditions are used to eliminate the rigid body modes of the element shape functions, define a unique displacement field, and establish the deformation basis vectors. By imposing the reference conditions, one can write $\mathbf{e}_{bf}$ in terms of a new reduced set of body nodal coordinates $\mathbf{e}_f$ as $\mathbf{e}_{bf} = \mathbf{B}_r \mathbf{e}_f$, where $\mathbf{B}_r$ is the matrix of reference conditions that eliminates dependent nodal coordinates and defines how the deformation is measured with respect to the body coordinate system. The number of reference conditions should not be less than the number of the rigid body modes of the finite element shape function. The position vector $\overline{\mathbf{u}}^j$ of the material point on the finite element can then be defined in the body coordinate system as

$$\overline{\mathbf{u}}^j = \mathbf{S}_b^j \mathbf{B}_c^j \left(\mathbf{e}_{bo} + \mathbf{B}_r \mathbf{e}_f \right), \qquad j = 1, 2, \ldots n_e \tag{2}$$

This position vector can be written as the sum of the position vector in the undeformed state plus the deformation vector as $\overline{\mathbf{u}}^j = \overline{\mathbf{u}}_o^j + \overline{\mathbf{u}}_f^j$, $j = 1, 2, \ldots n_e$, where $\overline{\mathbf{u}}_o^j = \mathbf{S}_b^j \mathbf{B}_c^j \mathbf{e}_{bo}$ and $\overline{\mathbf{u}}_f^j = \mathbf{S}_b^j \mathbf{B}_c^j \mathbf{B}_r \mathbf{e}_f$. Using Eqs. 1 and 2, one can write

$$\mathbf{r}^j = \mathbf{r}_O + \mathbf{A} \left(\overline{\mathbf{u}}_o^j + \overline{\mathbf{u}}_f^j \right), \qquad j = 1, 2, \ldots, n_e \tag{3}$$

Using this equation and the principle of virtual work, one can show that the FE/FFR equations of motion of the deformable body can be written as $\mathbf{M}\ddot{\mathbf{q}} = \mathbf{Q}_s + \mathbf{Q}_e + \mathbf{Q}_v$, where $\mathbf{q} = \begin{bmatrix} \mathbf{q}_r^T & \mathbf{q}_f^T \end{bmatrix}^T$ is

the vector of the body coordinate, $\mathbf{q}_r$ is the vector of reference coordinates, $\mathbf{q}_f$ is the vector of deformation (elastic) coordinates, $\mathbf{M}$ is the body mass matrix, $\mathbf{Q}_s$ is the vector of elastic (stress) forces, $\mathbf{Q}_e$ is the vector of external forces, and $\mathbf{Q}_v$ is the vector of Coriolis and centrifugal forces. Using the coordinate partitioning $\mathbf{q} = \begin{bmatrix} \mathbf{q}_r^{\mathrm{T}} & \mathbf{q}_f^{\mathrm{T}} \end{bmatrix}^{\mathrm{T}}$, the preceding equation can be written as

$$\begin{bmatrix} \mathbf{M}_{rr} & \mathbf{M}_{rf} \\ \mathbf{M}_{fr} & \mathbf{M}_{ff} \end{bmatrix} \begin{bmatrix} \ddot{\mathbf{q}}_r \\ \ddot{\mathbf{q}}_f \end{bmatrix} = \begin{bmatrix} \mathbf{0} \\ (\mathbf{Q}_s)_f \end{bmatrix} + \begin{bmatrix} (\mathbf{Q}_e)_r \\ (\mathbf{Q}_e)_f \end{bmatrix} + \begin{bmatrix} (\mathbf{Q}_v)_r \\ (\mathbf{Q}_v)_f \end{bmatrix} \tag{4}$$

The vector and matrices that appear in this equation are the assembled FE vectors and matrices, subscripts r and f refer, respectively, to reference and elastic coordinates, $\mathbf{q}_r = \begin{bmatrix} \mathbf{r}_O^{\mathrm{T}} & \boldsymbol{\theta}^{\mathrm{T}} \end{bmatrix}^{\mathrm{T}}$, and $\mathbf{q}_f = \mathbf{e}_f$.

3.3   Choice of the Reference Conditions

One of the main goals of this investigation is to use a simple single degree of freedom analytical model to show that no one set of deformation basis vectors is suited for all applications. When the FE/FFR formulation is used, the definition of a unique displacement field defines a subspace (Agrawal and Shabana, 1985; Shabana, 1996), and each set of reference conditions defines a different coordinate system and different subspace and convergence should only be judged within this subspace. Improper choice of the reference conditions can lead to wrong solutions as will be demonstrated in this investigation. In this paper, we differentiate between the FFR reference conditions and structural mechanics boundary conditions. The structural mechanics boundary conditions eliminate degrees of freedom, while the FFR reference conditions eliminate coordinate redundancy. In the FFR analysis, degrees of freedom can be eliminated using the MBS joint constraints. It is also important to recognize that sub-structuring techniques used for a

13

system assembly do not impose boundary conditions and the Craig-Bampton interface constraints should not be viewed as boundary conditions or reference conditions as discussed in the literature (O'Shea et al, 2016). Different sets of reference conditions, however, can lead to similar deformation shapes and solutions that are in a good agreement as previously demonstrated in the literature (Agrawal and Shabana, 1985; Shabana, 1996).

After imposing the reference conditions, which define the nature of the body coordinate system, one can use the *normal mode approach*, which is a general, convenient, and straight forward approach for determining the deformation basis vectors. Using component mode reduction techniques, the vector of the body coordinates can be written in terms of another smaller set of coordinates, thereby significantly reducing the problem dimensionality and eliminating high frequency modes that do not have significant effect on the solution accuracy. In order to use the component mode techniques, the free vibration of the body with respect to its reference is first considered. In this case, one has $\mathbf{M}_{ff}\ddot{\mathbf{q}}_f + \mathbf{K}_{ff}\mathbf{q}_f = \mathbf{0}$. One can assume a solution of this equation in the form $\mathbf{q}_f = \mathbf{a}e^{i\beta t}$, where $i = \sqrt{-1}$, $\mathbf{a}$ is the vector of amplitude, t is time, and β is the frequency. Substituting this assumed solution in the preceding free-vibration equation, one obtains the *generalized eigenvalue problem* $\left(\mathbf{K}_{ff} - \beta^2 \mathbf{M}_{ff}\right)\mathbf{a} = \mathbf{0}$. This equation can be solved for the eigenvalues β_k^2, $k = 1, 2, \ldots, n_f$, where n_f is the number of elastic nodal coordinates. The *eigenvectors* or *mode shapes* associated with the eigenvalues β_k^2 can also be determined. Using the eigenvectors, a constant coordinate transformation from the physical nodal coordinates $\mathbf{q}_f$ to the new modal elastic coordinates $\mathbf{p}_f$ can then be written as $\mathbf{q}_f = \mathbf{B}_m\mathbf{p}_f$, where $\mathbf{B}_m$ is the *modal transformation matrix* whose columns are the low-frequency n_m mode

shapes, and $\mathbf{p}_f$ is the reduced vector of modal coordinates. The total vector of the body coordinates can be written in terms of the new reduced set of coordinates as

$$\mathbf{q} = \begin{bmatrix} \mathbf{q}_r \\ \mathbf{q}_f \end{bmatrix} = \begin{bmatrix} \mathbf{I} & \mathbf{0} \\ \mathbf{0} & \mathbf{B}_m \end{bmatrix} \begin{bmatrix} \mathbf{p}_r \\ \mathbf{p}_f \end{bmatrix} \tag{5}$$

Substituting this transformation into the equations of motion and pre-multiplying by the transpose of the coefficient matrix in the coordinate transformation of the preceding equation leads to

$$\begin{bmatrix} \mathbf{M}_{rr} & \overline{\mathbf{M}}_{rf} \\ \overline{\mathbf{M}}_{fr} & \overline{\mathbf{M}}_{ff} \end{bmatrix} \begin{bmatrix} \ddot{\mathbf{p}}_r \\ \ddot{\mathbf{p}}_f \end{bmatrix} + \begin{bmatrix} \mathbf{0} & \mathbf{0} \\ \mathbf{0} & \overline{\mathbf{K}}_{ff} \end{bmatrix} \begin{bmatrix} \mathbf{p}_r \\ \mathbf{p}_f \end{bmatrix} = \begin{bmatrix} (\mathbf{Q}_e)_r \\ (\overline{\mathbf{Q}}_e)_f \end{bmatrix} + \begin{bmatrix} (\mathbf{Q}_v)_r \\ (\overline{\mathbf{Q}}_v)_f \end{bmatrix} \tag{6}$$

In this equation,

$$\left. \begin{array}{l} \overline{\mathbf{M}}_{rf} = \overline{\mathbf{M}}_{fr}^{\mathrm{T}} = \mathbf{M}_{rf} \mathbf{B}_m , \qquad \overline{\mathbf{M}}_{ff} = \mathbf{B}_m^{\mathrm{T}} \mathbf{M}_{ff} \mathbf{B}_m \\ \overline{\mathbf{K}}_{ff} = \mathbf{B}_m^{\mathrm{T}} \mathbf{K}_{ff} \mathbf{B}_m , \quad (\overline{\mathbf{Q}}_e)_f = \mathbf{B}_m^{\mathrm{T}} (\mathbf{Q}_e)_f , \quad (\overline{\mathbf{Q}}_v)_f = \mathbf{B}_m^{\mathrm{T}} (\mathbf{Q}_v)_f \end{array} \right\} \tag{7}$$

As discussed in the literature, the FE/FFR equations of motion can be expressed in terms of constant shape integrals that depend on the assumed displacement field. These constant shape integrals can be expressed in their modal form at a preprocessing stage using the modal transformation in order to reduce the array size required during the dynamic simulation.

4. DEFORMATION BASIS VECTORS

In order to be able to develop the simple analytical model used in this investigation to demonstrate analytically and numerically that one set of deformation basis vectors cannot be used for all applications, a set of reference conditions that will be used later in this paper to define a single-degree of freedom linear model is discussed in this section. The single-degree-of-

freedom model developed in this study can be used to shed light on fundamental issues related to the implementation of the FE/FFR formulation and its use in the durability analysis.

In the FE/FFR formulation, the large displacement is defined by the motion of the body reference. In the case of small deformation or simple deformation shapes, the use of the body coordinate system allows for creating a local linear problem that can be exploited to reduce systematically the number of coordinates by eliminating insignificant high frequency modes as described in the preceding section. Introducing the body coordinate system is also necessary when conventional finite elements that employ infinitesimal rotations are used. These elements cannot describe correctly finite rotations that must to be accurately represented in MBS computational algorithms that are based on non-incremental solution procedures. In order to define a unique displacement field, therefore, the rigid body motion of the FE shape functions must be eliminated. This is accomplished as discussed in the preceding section using the reference conditions that define the nature of the body coordinate system and define the deformation basis vectors. In MBS dynamics, the shape of deformation must be consistent with the MBS joint constraints imposed on the boundary of the deformable body. As will be demonstrated in the following sections of this paper, there is no single set of reference conditions and deformation basis vectors that is suited for all applications. For example, some commercial codes recommends that the users should not impose any reference (boundary) conditions and use free-free deformation modes after eliminating the rigid body zero-frequency modes. It is important to recognize that the free-free deformation modes correspond to a set of reference conditions called the *mean-axis conditions*. The mean-axis reference conditions are defined by the following set of equations (Ashley, 1967; Canavin and Likins, 1977; Likins, 1973; Agrawal and Shabana, 1985):

$$\int_V \rho \bar{\mathbf{u}}_f dV = 0, \qquad \int_V \rho \bar{\mathbf{r}} \times \bar{\mathbf{u}}_f dV = 0 \qquad (8)$$

In this equations, ρ and V are, respectively, the body mass density and volume, $\bar{\mathbf{u}}_f$ is the deformation vector, and $\bar{\mathbf{r}} = \bar{\mathbf{r}}\left(\mathbf{e}_{bo}, \mathbf{e}_f\right)$ is the position of the arbitrary point with respect to the body coordinate system. In order to have a linear equation, in the second equation of Eq. 8, $\bar{\mathbf{r}}$ is evaluated in the reference configuration, that is, $\bar{\mathbf{r}} = \bar{\mathbf{r}}\left(\mathbf{e}_{bo}\right)$. Using the preceding equation, one can develop the transformation $\mathbf{e}_{bf} = \mathbf{B}_r \mathbf{e}_f$ used in Section 3 of this paper to define a unique displacement field.

It has been shown in the literature that the use of the mean-axis reference conditions leads to the free-free deformation modes. That is, the free-free deformation modes after eliminating the rigid body zero-frequency modes correspond to a unique set of reference conditions. If the origin of the body coordinate system is initially located at the body center of mass, it can be shown that the mean-axis conditions ensure that the origin of the body coordinate system remains at the center of mass throughout the simulation. This is a case of a floating coordinate system since the resulting body reference is not necessarily attached to a material point on the body. The free-free deformation modes, however, produce specific geometry for the deformed shape that may not be suitable for all applications as will be demonstrated in this paper. Therefore, a MBS computer program that restricts the choice of the deformation modes to the free-free modes lacks generality and cannot be used as a general-purpose flexible MBS computer program.

As the result of assuming $\bar{\mathbf{r}} = \bar{\mathbf{r}}\left(\mathbf{e}_{bo}\right)$ in order to achieve linearity of the mean axis conditions, these conditions do not lead to a complete elimination of the dynamic coupling between the reference motion and the elastic deformation; weak inertia coupling still exists between the reference rotation and the elastic deformation of the body. Nonetheless, these

17

conditions can be effectively used to develop a new analytical linear model that leads to closed-form expressions which will shed light on fundamental issues including the appropriateness of using one set deformation basis vectors, effect of the MBS joints on the frequency contents of the solution, change in the resonance frequencies as the results of imposing the MBS joint constraints, appropriateness of the automatic elimination of redundant constraints as implemented in some MBS algorithms, etc.

5. FE AND MBS APPROACHES: FUNDAMENTAL DIFFERENCES

In this section, the simple model shown in Fig. 2 is used to develop reference solutions that will be used in this investigation to examine the effect and appropriateness of using different references conditions. The beam shown in the figure is assumed to be connected by pin joints at points O and A. The beam is subjected to a vertical force F as shown in the figure. The solutions will be obtained using two different algorithms and software. The first is a conventional FE approach and the second is a MBS approach. The basic features of the two approaches are described below.

1. **FE Approach**   In the FE approach, boundary conditions at points O and A are used in the general-purpose FE computer program **ANSYS**. Two different sets of boundary conditions are used; simply-supported and pinned-pinned. If u and v refer, respectively, to axial and bending deformations, the three simply-supported boundary conditions are $u_O = v_O = v_A = 0$, where subscripts refer to the points. In the case of pinned-pinned beam, the four boundary conditions are $u_O = v_O = u_A = v_A = 0$. A linear dynamic analysis is performed for the two models.

18

2. **MBS Approach**   In the MBS approach, the solutions are obtained for the same beam model

using the general-purpose MBS computer program **Sigma/Sams** (**S**ystematic **I**ntegration of

Geometric **M**odeling and **A**nalysis for the **S**imulation of **A**rticulated **M**echanical **S**ystems).

As previously mentioned in the paper, the reference conditions should not be interpreted, in

general, as boundary conditions. Boundary conditions eliminate degrees of freedom, while

reference conditions are used to eliminate the rigid body coordinate redundancy. Three

different sets of reference conditions are used in the MBS analysis of the model shown in

Fig. 2. The first set, the free-free modes, corresponds to the mean-axis conditions previously

discussed in this paper. The second set of reference conditions is referred to as the simply-

supported reference conditions ($u_O = v_O = v_A = 0$), and the third set of reference conditions is

referred to as the pinned-pinned reference conditions ($u_O = v_O = u_A = v_A = 0$). In the MBS

analysis, the following specific steps are followed: (1) An FE discretization is developed in a

preprocessor computer program in which the reference conditions are applied to define a

unique displacement field; (2) The resulting eigenvalue problem discussed in Section 3 is

used to determine the normal modes for each set of the reference conditions; (3) The shape

integrals are evaluated and expressed in their modal form (Shabana, 2013); (4) The

preprocessor prepares a file that includes the shape integrals and is used as an input to the

main processor; (5) The MBS pin joint constraints are imposed in the MBS model leading to

four algebraic equations, which are in general formulated using nonlinear equations. It is

clear, therefore, that both the reference conditions and the MBS pin joints must be

introduced. The reference conditions define a unique displacement field and define the nature

of the body coordinate system, while the MBS pin joint constraints eliminate kinematic

degrees of freedom and define the system topology.

The fundamental differences between the FE and the MBS approaches are clear from the discussion above. By introducing the body coordinate system, the MBS approach allows, in general, for describing finite rotations using a non-nodal set of coordinates. This allows for describing large displacements non-incrementally using conventional elements which are not capable of describing finite rotations.

The beam model shown in Fig. 2 is assumed to have mass $m = 0.1135$ kg, length $l = 0.4572$ m, density $\rho = 7.84 \times 10^3$ kg/m^3, circular cross-section with radius of 3.175×10^{-3} m, and modulus of elasticity $E = 2.0684 \times 10^{11}$ Pa. The beam is divided into 12 identical planar beam elements; each of which has two nodes and each node has three coordinates, two translations and one infinitesimal rotation. The force $F = -300$ N is assumed to apply at the fifth node which is assumed to have an initial displacement equivalent to -9.1669×10^{-3} m; this initial displacement is used to define the initial value of the modal coordinates. Figure 3 shows the normal modes that result from imposing the three different sets of reference conditions. The associated frequencies and the body coordinate systems are also shown in this figure. In all cases, the body coordinate system is not rigidly attached to a material point since translation and/or rotation is allowed with respect to the body coordinate system.

Figure 4 shows the transverse displacement of the beam at the point of the load application. The results presented in Fig. 4 are obtained using the commercial software ANSYS in the case of the two sets of simply-supported and pinned-pinned boundary conditions. Figure 5 shows the transverse displacement of the free-end of the beam when the two sets of boundary conditions are used. The axial displacement at point A is not zero when the simply-supported boundary conditions are used, while it is zero when the pinned-pinned boundary conditions are used. It was found, however, for this example that the axial displacement in the case of the simply-supported

boundary conditions is very small. In the conventional FE approach, the free-free end conditions cannot be used for this model; this fact is important to understand the fundamental difference between the structural mechanics boundary conditions and the FE/FFR reference conditions.

For the model shown in Fig. 2, the MBS approach allows using the free-free reference conditions. It was shown in the literature that in some applications, the free-free reference conditions can lead to solutions which are in a good agreement with the solutions obtained using other end conditions when the MBS approach is used (Agrawal and Shabana, 1985; O'Shea et al, 2016). Figure 6 shows the MBS and FE results of the transverse displacement of the point at which the load is applied. The results clearly show that for this extended beam model, the solution obtained using the free-free reference conditions does not converge to the solution obtained using the FE boundary conditions or other MBS reference conditions. Figure 7 shows the transverse displacement of the free end of the beam. The results presented in this figure show again that the solution obtained using the free-free reference conditions does not converge to the correct solution of the problem; the error as shown in Table 1 exceeds 100%, demonstrating that the use of improper reference conditions does not lead to reliable solution in any credible durability investigation.

The results presented in this section are obtained using two modes for each case. Convergence analysis was performed in order to ensure that higher modes do not have a significant effect on the accuracy of the solution. In summary, the results presented in this section demonstrate clearly the following:

1. Some sets of MBS reference conditions do not have equivalent structural mechanics boundary conditions. The system shown in Fig. 2 cannot be modeled using conventional FE free-free boundary conditions; it can, however, be modeled using the MBS free-free

21

reference conditions which in some applications can lead to a correct solution for constrained components as demonstrated in the literature (Agrawal and Shabana, 1985; O'Shea et al, 2016). For example, the free-free modes reference conditions can predict accurate solution if the beam is connected by pin joints at both ends, but cannot predict an accurate solution for the extended beam of Fig. 2.

2. While the MBS free-free reference conditions can give acceptable solution in some applications, as previously demonstrated in the literature, the use of this set of reference conditions can lead to a solution that converges to the wrong solution in some other applications as demonstrated by the results of the simple example considered in this section.

3. Different sets of reference conditions that are associated with different frequencies in the linear problem can lead to solutions that are in a good agreement.

In the following section, an analytical model is developed in order to shed light on some fundamental issues related to the constrained MBS dynamics.

6. ANALYTICAL MODEL

As mentioned in the preceding section, commercial FE computer programs cannot conveniently be used to verify the results obtained using the free-free MBS reference conditions for the model shown in Fig. 2. This makes clear the fundamental difference between the structural mechanics boundary conditions and the reference conditions used in flexible MBS analysis. The structural mechanics boundary conditions eliminate degrees of freedom, while the MBS reference conditions eliminate coordinate redundancy. Therefore, one must use another approach in order to verify the results obtained using the MBS simulations in the case of the free-free reference conditions. The results of the other sets of reference conditions (simply-supported and pinned-

pinned) have been already verified in the preceding section using the FE model. The MBS simulation results presented in the preceding section are obtained using the augmented Lagrangian formulation in which the MBS joint constraints are formulated using nonlinear algebraic equations that are adjoined to the system differential equations of motion using the technique of Lagrange multipliers.

In this section, the general MBS equations presented in Section 3 and the free-free modes reference conditions are used with the *embedding technique* to develop an unconstrained single-degree of freedom analytical model that can be used to shed light on the numerical results obtained in the preceding section and investigate fundamental issues related to the constrained motion of flexible bodies. In particular, the analytical results can be used to confirm the fact that the free-free end conditions lead to a wrong solution and such a set of reference conditions is not suited for all applications, including the very simple example considered in this study. The closed form equations obtained will be also used to discuss some fundamental durability analysis issues.

6.1 Single-Degree of freedom Analytical Model

In the modal transformation of Eq. 5, it is assumed that the contribution to the elastic nodal deformations of node k from mode m can be written as $\mathbf{q}_{fk} = \begin{bmatrix} \alpha_{km} & \beta_{km} & \gamma_{km} \end{bmatrix}^T p_{fm}$, where α_{km}, β_{km} and γ_{km}, are, respectively, the elements of the mode shape m associated with the axial displacement, transverse displacement, and rotation of the nodal point k; and p_{fm} is the amplitude (coordinate) of mode m. If only bending modes are used, one has $\alpha_{km} = 0$. We also note that in the case of a constant angular velocity, the vector $\mathbf{Q}_v$ of Eq. 4 is identically zero (Shabana, 2013; Sherif and Nachbagauer, 2014). This fact will be utilized in developing the analytical model presented in this section. In order to develop the single degrees of freedom

23

model, it is assumed that two deformation modes are used and the origin of the body coordinate system is initially located at point O. The distance between points O and A is denoted as d.

If free-free reference conditions, with two bending deformation modes, are used; the partitions of the modal matrix associated with the translations of points O and A of the model shown in Fig. 2 can be written as

$$\mathbf{S}_O = \begin{bmatrix} 0 & 0 \\ \beta_{O1} & \beta_{O2} \end{bmatrix}, \qquad \mathbf{S}_A = \begin{bmatrix} 0 & 0 \\ \beta_{A1} & \beta_{A2} \end{bmatrix} \tag{9}$$

The first rows in these two matrices are zero because of the use of bending deformation modes only. The four MBS pin joint constraint equations can be written in this case as

$$\mathbf{r}_O + \mathbf{A}\left(\bar{\mathbf{u}}_O + \mathbf{S}_O \mathbf{p}_f\right) = \mathbf{0}, \quad \mathbf{r}_O + \mathbf{A}\left(\bar{\mathbf{u}}_A + \mathbf{S}_A \mathbf{p}_f\right) - \mathbf{d} = \mathbf{0} \tag{10}$$

In this equation, $\bar{\mathbf{u}}_O$ and $\bar{\mathbf{u}}_A$ are, respectively, the local position vectors of points O and A in the reference configuration, $\mathbf{S}_O$ and $\mathbf{S}_A$ are, respectively, partitions of the modal transformation that correspond to the translational coordinates of points O and A, as previously defined, $\mathbf{d} = \begin{bmatrix} d & 0 \end{bmatrix}^T$, and

$$\bar{\mathbf{u}}_O = \mathbf{0}, \quad \bar{\mathbf{u}}_A = \begin{bmatrix} d \\ 0 \end{bmatrix}, \quad \mathbf{p}_f = \begin{bmatrix} p_{f1} \\ p_{f2} \end{bmatrix}, \quad \mathbf{A} = \begin{bmatrix} \cos\theta & -\sin\theta \\ \sin\theta & \cos\theta \end{bmatrix} \tag{11}$$

In this equation, p_{f1} and p_{f2} are the modal coordinates, and θ is the angle that defines the orientation of the body reference of the beam. Therefore, the MBS pin joint constraint equations reduce to

$$\mathbf{r}_O + \mathbf{A}\mathbf{S}_O \mathbf{p}_f = \mathbf{0}, \qquad \mathbf{r}_O + \mathbf{A}\left(\bar{\mathbf{u}}_A + \mathbf{S}_A \mathbf{p}_f\right) - \mathbf{d} = \mathbf{0} \tag{12}$$

Substituting the first equation into the second equation, one obtains

$$\mathbf{A}\left(\bar{\mathbf{u}}_A + \left(\mathbf{S}_A - \mathbf{S}_O\right)\mathbf{q}_f\right) - \mathbf{d} = \mathbf{0} \tag{13}$$

This equation can be used to show that for the example considered, $\cos\theta = 1$ or $\theta = 0$. To this end, the preceding equation is pre-multiplied by the transpose of the transformation matrix $\mathbf{A}$, leading to

$$\begin{bmatrix} d \\ \alpha_1 p_{f1} + \alpha_2 p_{f2} \end{bmatrix} = \begin{bmatrix} d\cos\theta \\ -d\sin\theta \end{bmatrix} \tag{14}$$

where $\alpha_1 = \beta_{A1} - \beta_{O1}$ and $\alpha_2 = \beta_{A2} - \beta_{O2}$. The first equation shows that $\cos\theta = 1$ or $\theta = 0$, while the second equation in the preceding equation yields $p_{f2} = -(\alpha_1/\alpha_2)p_{f1}$, which shows that the modal coordinates can be written in terms of one independent modal coordinate p_{f1} as

$$\begin{bmatrix} p_{f1} & p_{f2} \end{bmatrix}^T = \begin{bmatrix} 1 & \alpha_{12} \end{bmatrix}^T p_{f1}, \text{ where } \alpha_{12} = -(\alpha_1/\alpha_2). \text{ One can also show that } \mathbf{r}_O = \begin{bmatrix} 0 & \alpha_b \end{bmatrix}^T p_{f1},$$

where $\alpha_b = -(\beta_{O1} + \beta_{O2}\alpha_{12})$. Because two modes are considered, the vector of coordinates in Eq. 6 has 5 elements which can be written in terms of the independent modal coordinate p_{f1} as

$$\begin{bmatrix} r_{O1} & r_{O2} & \theta & p_{f1} & p_{f2} \end{bmatrix}^T = \begin{bmatrix} 0 & \alpha_b & 0 & 1 & \alpha_{12} \end{bmatrix}^T p_{f1} \tag{15}$$

The vector of forces $\mathbf{Q}_e$ in Eq. 6 can be written as

$$\mathbf{Q}_e = \begin{bmatrix} 0 & 1 & 0 & \alpha_{F1} & \alpha_{F2} \end{bmatrix}^T F \tag{16}$$

where β_{F1} and β_{F2} are the elements of the modal matrix that correspond to the transverse deformation at the point of the application of the vertical force F. One can also show that, for this system, the mass matrix in Eq. 6 is a 5×5 matrix that has the following structure:

$$\mathbf{M} = \begin{bmatrix} \mathbf{M}_{rr} & \bar{\mathbf{M}}_{rf} \\ \bar{\mathbf{M}}_{fr} & \bar{\mathbf{M}}_{ff} \end{bmatrix} = \begin{bmatrix} m & 0 & m_{13} & m_{14} & m_{15} \\ 0 & m & m_{23} & m_{24} & m_{25} \\ m_{13} & m_{23} & m_{33} & m_{34} & m_{35} \\ m_{14} & m_{24} & m_{34} & m_1 & 0 \\ m_{15} & m_{25} & m_{35} & 0 & m_2 \end{bmatrix} \tag{17}$$

where m is the total mass of the beam, m_{33} is the mass moment of inertia that depends on the beam deformation, m_1 and m_2 are the modal mass coefficients, $\begin{bmatrix} m_{13} & m_{23} \end{bmatrix}^T$ is the moment of mass vector which is constant in this case because of the mean-axis conditions and because $\theta = 0$, m_{34} and m_{35} represent the weak dynamic coupling between the rotation and deformation coordinates as the result of the application of the mean-axis conditions, and m_{14}, m_{15}, m_{24}, and m_{25} are the inertia coefficients that represent the coupling between the reference translation and the elastic modal coordinates; these coefficients are constant because $\theta = 0$ (Shabana, 2013; Sherif and Nachbagauer, 2014). Some of these coefficients need not to be defined explicitly because of the structure of the velocity transformation vector $\mathbf{B}_v = \begin{bmatrix} 0 & \alpha_b & 0 & 1 & \alpha_{12} \end{bmatrix}^T$ of Eq. 15. It is clear that

$$\mathbf{B}_v^T \mathbf{M} \mathbf{B}_v = \alpha_b^2 m + m_1 + \alpha_{12}^2 m_2 + 2\alpha_b m_{24} + 2\alpha_b \alpha_{12} m_{25} \tag{18}$$

The stiffness matrix $\overline{\mathbf{K}}_{ff}$ in Eq. 6 is diagonal with diagonal elements equal to the modal stiffness coefficients k_1 and k_2. Using the coordinate relationship developed in this section, $\theta = 0$, the fact that the mean-axis conditions eliminate the coupling between the body translation and the elastic deformation, and the fact that $\mathbf{B}_v^T$ eliminates the constraint forces, one can substitute Eq. 15 into Eq. 6 and pre-multiply by the transpose of the velocity transformation vector $\mathbf{B}_v = \begin{bmatrix} 0 & \alpha_b & 0 & 1 & \alpha_{12} \end{bmatrix}^T$ to obtain one equation which can be written as

$$\overline{m} \ddot{p}_{f1} + \overline{c} \dot{p}_{f1} + \overline{k} p_{f1} = \overline{Q} \tag{19}$$

In this equation,

$$\left. \begin{array}{l} \overline{m} = \mathbf{B}_v^T \mathbf{M} \mathbf{B}_v, \quad \overline{k} = k_1 + \alpha_{12}^2 k_2, \quad \overline{c} = c_1 + \alpha_{12}^2 c_2 \\ \overline{Q} = \left(\alpha_b + \beta_{F1} + \beta_{F2} \alpha_{12} \right) F \end{array} \right\} \tag{20}$$

26

where m_k, k_k, and c_k, $k = 1, 2$, are, respectively, modal mass, stiffness, and damping coefficients.

Equations 19 and 20 show the change in the system dynamics characteristics as the result of imposing the MBS joint constraints. As will be discussed in this section, the solution oscillation frequency for the above system is significantly different from the natural frequencies associated with the end conditions used to determine the mode shapes. The solution for p_{f1} can then be written in a closed form in the case of non-zero initial modal displacement $\left(p_{f1} \right)_0$ as

$$p_{f1} = X e^{-\bar{\xi}\bar{\omega}t} \sin\left(\bar{\omega}_d t + \phi\right) + \frac{\bar{Q}}{\bar{k}} \tag{21}$$

The symbols that appear in his equation, upon the use of the definition of the natural frequency $\bar{\omega} = \sqrt{\bar{k}/\bar{m}}$, can be written as

$$\bar{\xi} = \bar{c}/2\bar{m}_m\bar{\omega}_m, \quad \bar{\omega}_d = \bar{\omega}\sqrt{1-\bar{\xi}^2}, \quad X = \left(\left(p_{f1}\right)_0 - \frac{\bar{Q}}{\bar{k}}\right)\sqrt{\frac{1}{1-\bar{\xi}^2}}, \quad \phi = \tan^{-1}\frac{\sqrt{1-\bar{\xi}^2}}{\bar{\xi}} \tag{22}$$

In determining the equivalent damping coefficient $\bar{\xi}$, the free vibration of the body with respect to its coordinate system must be considered. That is, $\bar{m}_m = m_1 + \alpha_{12}^2 m_2 + 2\alpha_b m_{24} + 2\alpha_b\alpha_{12}m_{25}$ and $\bar{\omega}_m = \sqrt{\bar{k}/\bar{m}_m}$. The solution for p_{f1} can be used to determine p_{f2} from the equation $p_{f2} = -\left(\alpha_1/\alpha_2\right)p_{f1}$. Having determined the modal coordinates p_{f1} and p_{f2}, the displacement of the beam at an arbitrary point or node can be determined.

6.2 Verification of the Free-Free Mode Results

In the analysis of the simple model, it assumed that the mode shapes are orthogonal with respect to the stiffness matrix. That is, based on the model data previously presented, the modal mass and stiffness coefficients are given, respectively, by $m_1 = 0.131281 \times 10^5$, $m_2 = 0.172735 \times 10^{-06}$, $k_1 = 1$, and $k_2 = 1$. For all modes, a damping factor of

27

3% is used. The elements of the modal matrix used in the simple model equations are

$\beta_{O1} = -0.6802 \times 10^{-2}, \beta_{O2} = -0.2468 \times 10^{-2}, \beta_{A1} = 0.2521 \times 10^{-2}$ and $\beta_{A2} = -0.1603 \times 10^{-2}$. The

elements of the modal matrix at the point of the application of the force are $\beta_{F1} = 0.2521 \times 10^{-2}$

and $\beta_{F2} = 0.1603 \times 10^{-2}$. Figures 8 and 9 show, respectively, the transvers displacement at the

point of application of the force (Node 5) and the free end of the beam (Node 13) as functions of

time obtained using the analytical solution and the MBS computer program Sigma/Sams for

different reference conditions. It is clear that the free-free mode analytical solution agrees with

the free-free mode MBS solution, but both significantly differ from the FE solution which agrees

well with the MBS solution when the simply-supported or pinned-pinned reference conditions

are used. The results presented in Figs. 8 and 9 confirm the fact that the free-free modes are not

appropriate for all applications, including the simple example considered in this investigation.

Figure 10 shows the vertical displacement of the body reference in case of the free-free mode

reference conditions. The results of this figure, in which the analytical and MBS results are

compared, show that in the case of free-free reference conditions, the origin of the body

coordinate system does not remain at point O, while in the case of other reference conditions

considered in this paper, the origin of the body coordinate system remains at point O. In all

cases, however, the origin of the body coordinate system does not move in the axial direction

because of the kinematic constraints and because of using bending modes only. Figure 11, which

shows the deformed shape of the beam in the two cases of free-free and simply-supported end

conditions for the converged solution, clearly demonstrates the error in the free-free reference

conditions solution. With an inappropriate choice of the reference conditions, the deformation of

the beam can become very different in order to ensure that the MBS constraints are satisfied. It is

also clear from this figure that the second mode becomes significant and the body coordinate

28

system moves vertically in order to ensure that the MBS constraint equations are satisfied. The amplitude of the second mode can be claculated from the relationship $p_{f2} = \alpha_{12} p_{f1}$, where in this example $\alpha_{12} = -10.7756$. The elements that correspond to the two modes in the modal transformation matrix are approximately of the same order.

6.3 Reference Load Projection

The analysis of the single-degree of freedom model shows that the use of a systematic approach to obtain the independent deformation equation of motion leads to a definition of the generalized forces associated with the independent deformation degree of freedom. The generalized force $\overline{Q} = \left(\alpha_b + \beta_{F1} + \beta_{F2} \alpha_{12} \right) F$ includes a contribution from the external forces associated with the reference motion of the system. This contribution is defined by the term $\alpha_b F$ in the $\overline{Q}$ generalized force expression. In fact, this simple model reveals the very striking result that the contribution to the generalized force $\overline{Q} = \left(\alpha_b + \beta_{F1} + \beta_{F2} \alpha_{12} \right) F$ from the MBS reference load $\alpha_b F$, often ignored in the FE-based durability analysis, is approximately 4.8 times the contribution of the nodal forces $\left(\beta_{F1} + \beta_{F2} \alpha_{12} \right) F$; in this example $\left(\beta_{F1} + \beta_{F2} \alpha_{12} \right) = -0.412322/F$, while $\alpha_b = 1.978947/F$. That is, not only very different solution is obtained, but also the sign of the force and displacement will be reversed if the effect of the MBS reference load is not accounted for properly. Therefore, in FE-based durability analysis, it is not sufficient to distribute the forces on the nodal points without taking into account the MBS kinematic formulation. Most FE commercial software and algorithms, however, are not designed using a MBS approach.

6.4 Oscillation Frequency and Durability Analysis

The results of Figs. 8 and 9 show that the frequency of oscillation that appears in the free-free reference condition solution in the transient region is $\bar{\omega}_d = \bar{\omega}\sqrt{1-\bar{\xi}^2} = 1.3319\times10^3 \text{ rad/s} = 2.12\times10^2 \text{ Hz}$ rad/s, which is based on the natural frequency $\bar{\omega} = \sqrt{\bar{k}/\bar{m}} = 1.3322\times10^3$ rad/s. This MBS frequency is not related to the natural frequencies of the free-free modes presented in Fig. 3; it is, however, closer to the simply-supported and pinned-pinned second mode frequency. This important result clearly shows the change of the oscillation frequencies in the solution as the result of imposing the MBS joint constraints. The use of the embedding technique to eliminate the dependent variables and define an independent differential equation of motion leads to the projection of the inertia, damping, and stiffness forces in the direction of the degree of freedom of the system. Such a projection results in a change of the system inertia, damping, and stiffness characteristics. Accordingly, the resonance frequency can be significantly altered as the result of imposing the MBS joint constraints. This simple example, therefore, demonstrates the problems that can be encountered in a durability analysis that ignores the MBS joint constraints and relies mainly on a conventional FE analysis which does not account for the MBS joint constraints and does not allow for systematically using the projection scheme of the embedding technique as described in this paper.

It is important to point out that the use of loads predicted using MBS software as input to a conventional FE model does not remedy the problem discussed in this subsection. Loads are not kinematic joints, do not eliminate degrees of freedom, and do not alter the resonance frequencies. Therefore, the frequency contents in the solution will depend only on the FE boundary conditions, which are not in general equivalent to the MBS joint constraints. The MBS-predicted loads, when used in an FE durability analysis, do not change the deformation basis vectors and do not change the resonance ranges of the model. More reliance on accurate flexible MBS

30

computational tools is the solution for credible durability analysis of systems that consist of interconnected bodies.

7. AUTOMATIC ELIMINATION OF REDUNDANT CONSTRAINTS

The simple example considered in this investigation defines indeterminate (over-constrained) system if the effect of the deformation is not considered. A planar rigid body has three degrees of freedom if no constraints are imposed on its motion. The two pin-joints are defined using four algebraic constraint equations, leading to an over-constrained system if this system were rigid. By considering two bending modes of vibration, the system has one degree of freedom as demonstrated in the preceding example. This flexible body system is not topologically over-constrained. Nonetheless, singularity of the constraint Jacobian matrix can appear if the initial conditions are zeros and if no axial modes of vibration are considered. In order to demonstrate this initial configuration singularity, the constraint equations, $\mathbf{r}_O + \mathbf{AS}_O \mathbf{p}_f = \mathbf{0}$ and $\mathbf{r}_O + \mathbf{A}\left(\overline{\mathbf{u}}_A + \mathbf{S}_A \mathbf{p}_f\right) - \mathbf{d} = \mathbf{0}$ (Eq. 12), are differentiated with respect to the coordinates $\mathbf{r}_O, \theta$, and $\mathbf{p}_f$. This yields the following constraint Jacobian matrix:

$$\mathbf{J}_m = \begin{bmatrix} 1 & 0 & -\beta_O \cos\theta & -\beta_{O1}\sin\theta & -\beta_{O2}\sin\theta \\ 0 & 1 & -\beta_O \sin\theta & \beta_{O1}\cos\theta & \beta_{O2}\cos\theta \\ 1 & 0 & -\left(d\sin\theta + \beta_A \cos\theta\right) & -\beta_{A1}\sin\theta & -\beta_{A2}\sin\theta \\ 0 & 1 & d\cos\theta - \beta_A \sin\theta & \beta_{A1}\cos\theta & \beta_{A2}\cos\theta \end{bmatrix} \tag{23}$$

In this equation, $\beta_O = \beta_{O1}p_{f1} + \beta_{O2}p_{f2}$ and $\beta_A = \beta_{A1}p_{f1} + \beta_{A2}p_{f2}$. Because θ remains zero in this example, it is clear that in the case of zero initial modal coordinates, that is $\left(p_{f1}\right)_0 = \left(p_{f2}\right)_0 = 0$, one has $\beta_O = 0$ and $\beta_A = 0$, and the constraint Jacobian matrix becomes

31

$$\mathbf{J}_m = \begin{bmatrix} 1 & 0 & 0 & 0 & 0 \\ 0 & 1 & 0 & \beta_{O1} & \beta_{O2} \\ 1 & 0 & 0 & 0 & 0 \\ 0 & 1 & d & \beta_{A1} & \beta_{A2} \end{bmatrix} \tag{24}$$

This equation shows *initial-configuration singularity* since the first and third rows are identical. The MBS constraint Jacobian matrix becomes rank deficient despite the fact that the system is not topologically over-constrained. This simple example sheds light on the danger of automatic elimination of redundant constraints, which can lead to creating a new system topology that may lead to a different solution and different oscillation frequencies as discussed in the preceding section. In MBS algorithms, the constraint forces can be written in terms of the constraint Jacobian matrix $\mathbf{J}_m$ and the vector of Lagrange multipliers $\boldsymbol{\lambda}$ as $\mathbf{J}_m^T \boldsymbol{\lambda}$.

For the example considered in this investigation, $\theta = 0$, that is $\sin\theta = 0$ and $\cos\theta = 1$. Using Eq. 23, one can show that

$$\mathbf{J}_m = \begin{bmatrix} 1 & 0 & -\beta_O & 0 & 0 \\ 0 & 1 & 0 & \beta_{O1} & \beta_{O2} \\ 1 & 0 & -\beta_A & 0 & 0 \\ 0 & 1 & d & \beta_{A1} & \beta_{A2} \end{bmatrix} \tag{25}$$

Using the velocity transformation vector $\mathbf{B}_v = \begin{bmatrix} 0 & \alpha_b & 0 & 1 & \alpha_{12} \end{bmatrix}^T$, one can show that $\mathbf{B}_v^T \mathbf{J}_m^T \boldsymbol{\lambda} = 0$, demonstrating how the constraint equations are systematically eliminated to determine the analytical model.

8. SUB-STRUCTURING INTERFACE CONDITIONS

Another set of conditions that are widely used in the durability analysis of mechanical and structural systems is the sub-structuring interface conditions (Craig and Bampton, 1968; O'Shea

et al., 2016). There is a fundamental difference between these conditions and the structural mechanics boundary conditions and the FFR reference conditions. In sub-structuring techniques, the structure is divided into substructures at nodes, called the *interface* or *sub-structure boundary nodes*, which are used with a static condensation method to determine a set of basis vectors equal to the number of degrees of freedom of the interface nodes. These basis vectors, called *static correction modes*, can be systematically obtained by using stiffness sub-matrices while the effect of the structure inertia is neglected (Craig and Bampton, 1968, O'Shea et al., 2016). The interface nodes are then assumed fixed and an eigenvalue problem is solved for each sub-structure to determine its *interface deformation modes*. These interface deformation modes are combined with the static correction modes to form the Craig-Bampton transformation matrix. At this stage, the high frequency interface deformation modes can be eliminated in order to develop a low order model for each substructure. Using the reduced order substructure models, the substructures can be assembled using the connectivity conditions at the interface nodes, leading to a structure with a reduced order model as the result of reducing the dimensions of its substructures. Boundary conditions on the entire structure motion can be then imposed if necessary. In some of the aerospace applications, such as airplanes, no boundary conditions need to be imposed to eliminate additional degrees of freedom since airplanes are often modeled as free-free structures that have rigid body modes.

Craig and Bampton (1968) never claimed that such a sub-structuring procedure leads to an improvement of the solution, and never argued that the static correction modes will lead to such an improvement. Their goal was to demonstrate that their sub-structuring technique will lead to a solution that converges to the solution of the original problem, and by including sufficient number of sub-structuring modes, their technique does not lead to deterioration in the accuracy.

It is, therefore, important to note that the Craig-Bampton sub-structuring technique does not eliminate the rigid body motion of the structure since modeling free-free structures using sub-structuring techniques is very common in the aerospace industry.

Based on this brief discussion, the fundamental differences between the sub-structuring interface conditions, the structural mechanics boundary conditions, and the FFR reference conditions can be made clear from the following well-established facts:

1. The *sub-structuring interface conditions* do not eliminate rigid body modes, do not significantly change the fundamental frequencies of the assembled structure, and do not define the system topology because no joints are introduced. The sub-structuring interface conditions are mainly used to assemble substructures after the elimination of the sub-structure high frequency deformation modes. The Craig-Bampton transformation still accounts for the rigid body modes.

2. The *structural mechanics boundary conditions* eliminate rigid body modes, define the fundamental frequencies of the system, and define the system topology since joints are introduced to the model. This is evident by the fact that different boundary conditions lead to different solutions and natural frequencies. The boundary conditions are, for the most part, considered as joint constraints on structures that do not experience large rigid body displacement. If the structure has arbitrarily large displacements, the use of the concepts of the FFR formulation becomes necessary if an FE method capable of correctly describing the rigid motion is not used.

3. The *FFR reference conditions* eliminate the rigid body motion of the structure with respect to its reference, do not eliminate the rigid body modes of the structure, define the nature of the body coordinate system, define a unique displacement field and the shapes of deformation of

34

the flexible body with respect to its reference, do not influence the frequency contents in the solution since the flexible body still has its rigid body modes described by the reference coordinates, and do not change the system topology because the reference conditions are not mechanical joints. In the FFR formulation, the system topology is defined by the MBS joint constraints. The frequency contents in the solution is influenced by these MBS joint constraints as demonstrated by the simple analytical model considered in this paper.

Therefore, if additional conditions are imposed to eliminate the rigid body modes after obtaining the Craig-Bampton transformation, these conditions are either boundary conditions in the case of structural systems or FFR reference conditions in the case of MBS applications. In the latter case, mechanical joints that define the system topology and the frequency contents can be applied in order to assemble the system components. Nonetheless, the definition of a unique displacement field for each body is necessary before the system assembly using mechanical joints that are described for MBS applications using highly nonlinear algebraic equations instead of the linear boundary conditions often used for structural mechanics applications.

9. SUMMARY AND CONCLUSIONS

In this investigation, simple numerical and analytical models are used to address fundamental FE/FFR implementation issues. The reference solutions used are confirmed using a full FE analysis. The new models can, therefore, serve as a benchmark examples that shed light on some serious problems encountered in performing the durability analysis by the industry. The issues addressed and the contributions made in this paper can be summarized as follows:

1. The analysis presented in this paper demonstrates that one set of reference conditions is not suited for all applications. Consequently, the generality of the FE/FFR formulation can be

35

severely limited by restricting the choice of the *reference conditions* to one set. This important fact was confirmed by developing a new analytical model that demonstrated the problems that arise if general-purpose flexible MBS computer programs restrict the choice of the deformation basis vectors. The new analytical model, supported by MBS simulation data, shows that such a restriction can lead to wrong solutions in the case of very simple models.

2. The paper demonstrates the fundamental difference between the boundary conditions used in the classical vibration theory and structural mechanics and the reference conditions used in MBS dynamics. Structural mechanics boundary conditions eliminate degrees of freedom, while the FE/FFR reference conditions eliminate coordinate redundancy and define a unique displacement field. Some sets of MBS reference conditions do not have equivalent boundary conditions in structural mechanics, as demonstrated by the simple model considered in this study. The differences between the structural mechanics boundary and FFR reference conditions and the sub-structuring interface conditions were also explained.

3. When the MBS constraints are applied, use of inappropriate set of reference conditions can lead to wrong solutions. Because low-frequency modes with simpler shapes may fail to satisfy the MBS algebraic constraint equations, modes associated with higher frequencies may become more dominant as demonstrated by the analytical model developed in this paper. As shown in Table 1, the improper selection of the reference conditions can lead to solution errors that exceed 100%, making such a solution completely unreliable.

4. It is common that CAE groups in the industry perform durability FE analysis using FE boundary conditions. The analysis presented in this paper sheds light on the credibility of using this approach. It is shown that MBS joints change the model dynamics characteristics, including the inertia, damping, and forces as well as the resonance frequencies. Therefore,

36

the durability analysis must be performed in a MBS computational environment in order to correctly capture the effect of the MBS kinematic constraints and ensure proper projection of the forces that produce the deformations and stresses. In particular, the analysis presented in this paper shows that the contribution of the reference forces to the independent deformation coordinates requires the formulation of the MBS joint constraints which are not included in commercial FE computer programs.

5. The frequencies of oscillation and the resonance ranges of one component of the system based on linear analysis can be significantly different from those of the assembled MBS model. That is, the frequencies predicted for a component using detailed FE analysis should not enter as a factor in the design of the assembled component which can experience arbitrarily large displacements.

6. Some commercial MBS computer programs provide the feature of the automatic removal of redundant constraints. In some cases, as demonstrated in this paper, automatic elimination of redundant constraints can lead to a different model that has dynamics characteristics that are significantly different from those of the original model. It is important, therefore, to distinguish between *topological singularities* and *initial-configuration singularities*.

Future investigations in this area can be focused on further studies of the initial-configuration singularities, and developing analytical models with more degrees of freedom to include other types of modes such as axial modes. These analytical models can be valuable in clearly explaining the projection of forces and addressing important durability analysis issues.

37

REFERENCES

1. Agrawal, O.P., and Shabana, A.A., 1985, "Dynamic Analysis of Multibody Systems Using Component Modes", *Computers & Structures*, Vol. 21(6), pp. 1303-1312.

2. Ashley, H., 1967, "Observations on the Dynamic Behavior of Large Flexible Bodies in Orbit", *AIAA Journal*, Vol. 5, pp. 460 – 469.

3. Bahgat, B., and Willmert, K.D., 1973, "Finite Element Vibration Analysis of Planar Mechanisms". *Mech. Machine Theory*, Vol. 8, pp. 497–516.

4. Canavin, J.R., and Likins, P.W., 1977, "Floating Reference Frames for Flexible Spacecraft", *J. Spacecr. Rockets*, Vol. 14, pp. 724–732.

5. Chu, S.C., and Pan, K.C., 1975, "Dynamic Response of a High-Speed Slider Crank Mechanism with an Elastic Connecting Rod", *ASME J. Eng. Industry*, Vol. 92, pp. 542–550.

6. Craig Jr., R.R., and Bampton, M.C.C., 1968, "Coupling of Substructures for Dynamic Analyses", *AIAA Journal*, Vol. 6(7), pp. 1313-1319.

7. Erdman, A.G., and Sandor, G.N., 1972, "Kineto-Elastodynamics: A Review of the State of the Art and Trends", *Mech. Machine Theory*, Vol.7, pp.19–33.

8. Hegazy, S., Rahnejat, H., and Hussain, K., 1999, "Multi-Body Dynamics in Full-Vehicle Handling Analysis", *Proc. Inst. Mech. Engrs. Part K J. Multi-body Dynam.*, Vol. 213, pp. 19–31.

9. Ho, J.Y.L., 1977, "Direct Path Method for Flexible Multibody Spacecraft Dynamics", *J. Spacecraft Rockets*, Vo. 14, pp. 102–110.

10. Ho, J.Y.L., and Herber, D.R., 1985, "Development of Dynamics and Control Simulation of Large Flexible Space Systems", *J. Guidance Control Dynam.*, Vol. 8, pp. 374–383.

11. Hooker, W.W., 1975, "Equations of Motion of Interconnected Rigid and Elastic Bodies", *Celest. Mech.*, Vol. 11, pp. 337–359.

12. Jerkovsky, W., 1978, "The Structure of Multibody Dynamics Equations", *J. Guidance Control*, Vol. 1, pp. 173–182.

13. Kane, T.R., and Levinson, D.A., 1983, "Multibody dynamics", *ASME J. Appl. Mech.*, Vol. 50, pp. 1071–1078.

14. Kane, T.R., and Levinson, D.A., 1985, *Dynamics: Theory and applications*, McGraw-Hill, New York.

15. Kushwaha, M., Gupta, S., Kelly, P., and Rahnejat, H., 2002, "Elasto-Multi-Body Dynamics of a Multicylinder Internal Combustion Engine", *Proc. Inst. Mech. Engrs. Part K J. Multibody Dynam.*, Vol. 216, pp. 281–293.

16. Likins, P.W., 1973, "Dynamic Analysis of a System of Hinge-Connected Rigid Bodies with Nonrigid Appendages", *Int. J. Solids Struct.*, Vol. 9, pp.1473–1487.

17. Liu, C., Tian, Q., and Hu, H., 2011, "Dynamics of a Large Scale Rigid-Flexible Multibody System Composed of Composite Laminated Plates", *Multibody System Dynamics*, Vol. 26, pp. 283–305.

18. Lowen, G.G., and Chassapis, C, 1986, "The Elastic Behavior of Linkages: An Update", *Mech. Machine Theory*, Vol. 21, pp. 33–42.

19. Lowen, G.G., and Jandrasits, W.G., 1972, "Survey of Investigations into the Dynamic Behavior of Mechanisms Containing Links with Distributed Mass and Elasticity", *Mech. Machine Theory*, Vol. 7, pp. 13–17.

20. Magnus, K., 1978, *Dynamics of Multibody Systems,* Springer Verlag, Berlin.

21. O'Shea, J.J., Jayakumar, P., Mechergui, D., Shabana, A.A., and Wang, L., 2016, "Substructuring Techniques and Reference Conditions in Flexible Multibody System Dynamics", Technical Report # MBS2016-5-UIC, Department of Mechanical Engineering, The University of Illinois at Chicago, September 2016.

22. Orlandea, N., Chace, M.A., and Calahan, D.A., 1977, "A Sparsity-Oriented Approach to Dynamic Analysis and Design of Mechanical Systems", *ASME J. Eng. Industry*, Vol. 99, pp. 773–784.

23. Rahnejat, H., 2000, "Multi-Body Dynamics: Historical Evolution and Application", *Proc. Inst. Mech. Engrs. Part C J. Mech. Eng. Sci.*, Vol. 214, pp. 149–173.

24. Roberson, R.E., and Schwertassek, R., 1988, *Dynamics of Multibody Systems*, Springer Verlag, Berlin.

25. Sadler, J.P., and Sandor, G.N., 1973, "A lumped Approach to Vvibration and Stress Analysis of Elastic Linkages", *ASME J. Eng. Industry*, Vol. 95, pp. 549–557.

26. Schiehlen, W.O., 1982, "Dynamics of Complex Multibody Systems", *SM Arch.*, Vol. 9, pp. 297–308.

27. Shabana, A.A., 1996, "Resonance Conditions and Deformable Body Co-ordinate Systems", *Journal of Sound and Vibration,* Vol. 192(1), pp. 389-398.

28. Shabana, A.A., 2013, *Dynamics of Multibody Systems*, Third Edition, Cambridge University Press, Cambridge, UK.

29. Sherif, K., Nachbagauer, K., 2014, "A Detailed Derivation of the Velocity-Dependent Inertia Forces in the Floating Frame of Reference Formulation", *ASME Journal of Computational and Nonlinear Dynamics*, Vol. 9, doi: 10.1115/1.4026083, pp. 044501-1- 044501-8.

30. Sunada, W., and Dubowsky, S., 1981, "The Application of the Finite Element Methods to the Dynamic Analysis of Flexible Spatial and Co-planar Linkage Systems", *ASME J. Mech. Design*, Vol. 103, pp. 643–651.

31. Sunada, W., and Dubowsky, S., 1983, "On the Dynamic Analysis and Behavior of Industrial Robotic Manipulators with Elastic Members', *ASME J. Mech. Transmissions Automation Design*, Vol. 105, pp. 42–51.

32. Turcic, D.A., and Midha, A., 1984, "Dynamic Analysis of Elastic Mechanism Systems, parts I & II", *ASME J. Dynam. Syst. Measurement Control*, Vol. 106, pp. 249–260.

33. Udwadia, F.E., and Schutte, A.D., 2010, "Equations of Motion for General Constrained Systems in Lagrangian Mechanics", *Acta Mechanica*, Vol. 213, pp. 111–129.

34. Udwadia, F.E., and Wanichanon, T., 2010, "Hamel's Paradox and the Foundations of Analytical Dynamics", *Applied Mathematics and Computations*, Vol. 217, pp. 1253–1263.

35. Wittenburg, J. 1977, *Dynamics of Systems of Rigid bBodies*, Teubner, Stuttgart.

LIST OF FIGURES

Table 1 Converged values and percentage error

Node	Free-free sol. (m)	Simply-supported sol. (m)	Percentage error
Load node	-3.0557×10^{-3}	-1.0719×10^{-2}	71.5%
Free end	-4.7052×10^{-3}	1.6081×10^{-2}	129.3%
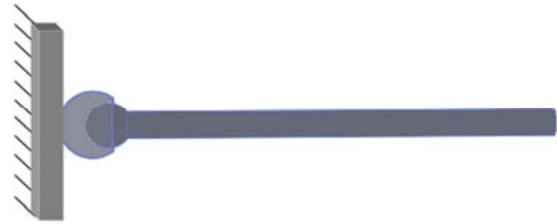
(a) Planar pendulum   (b) Spherical pendulum

Figure 1 Planar and spherical pendulums

$F = 300$N

O A

Figure 2 Beam model

$\omega = 138.91$

$\omega = 382.94$

(a) Free-Free

$\omega = 88.64$

$\omega = 209.4$

(b) Simply-Supported

$\omega = 88.64$

$\omega = 209.4$
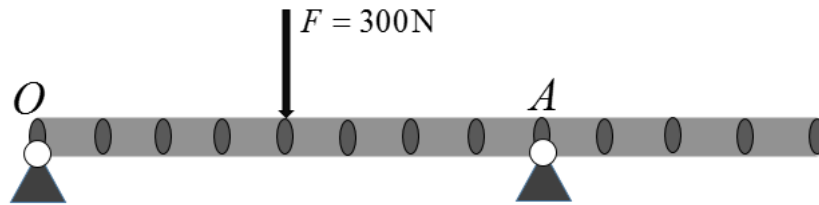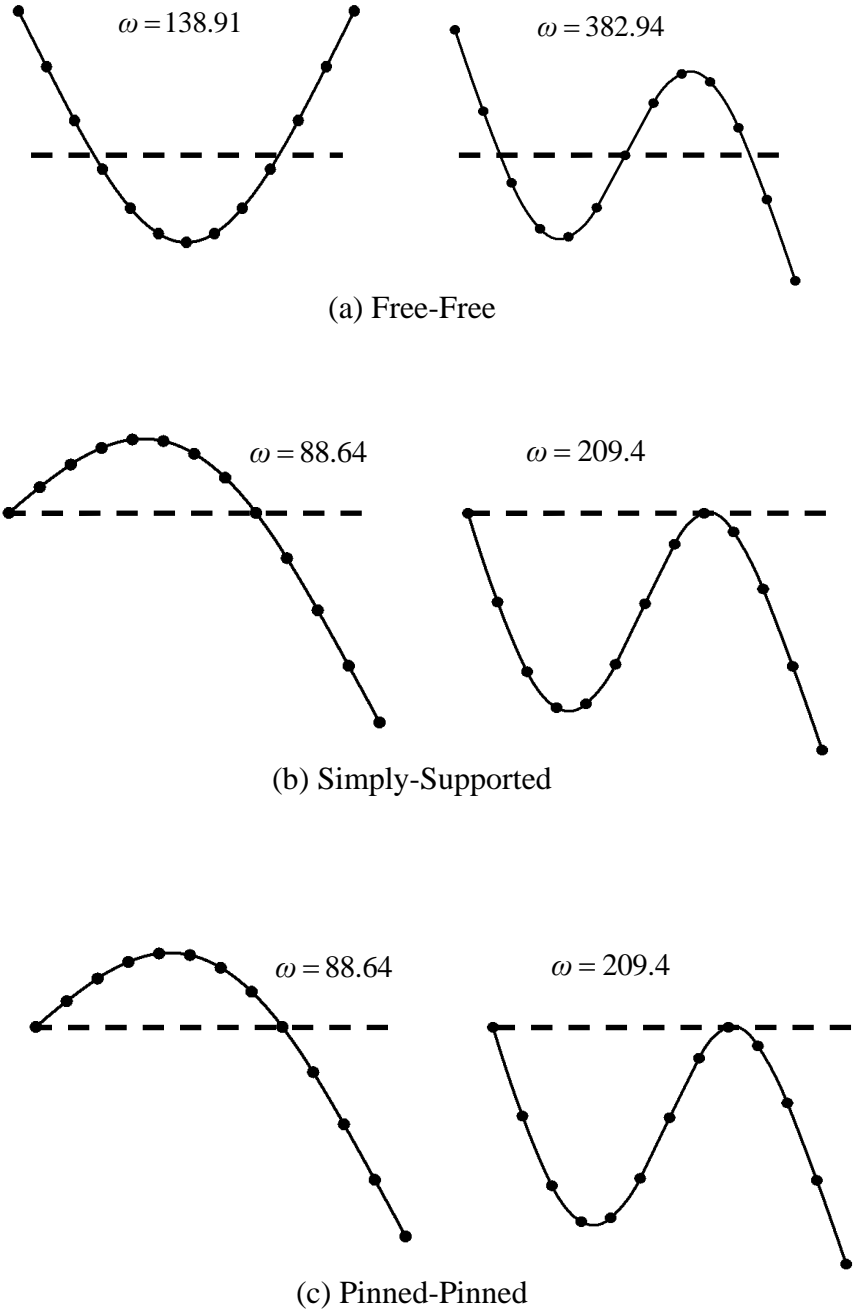
(c) Pinned-Pinned

Figure 3 Mode shapes and associated frequencies in Hz
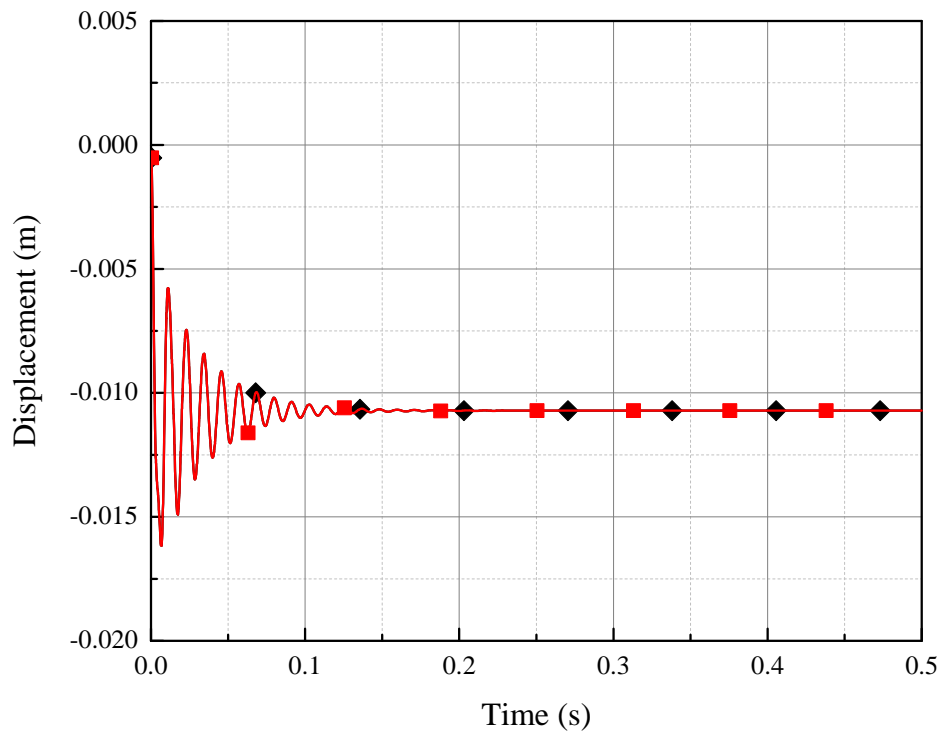
Figure 4 Transverse displacement at the point of the load application predicted using FE method
(━◆━ Simply-Supported, ━■━ Pinned-Pinned)
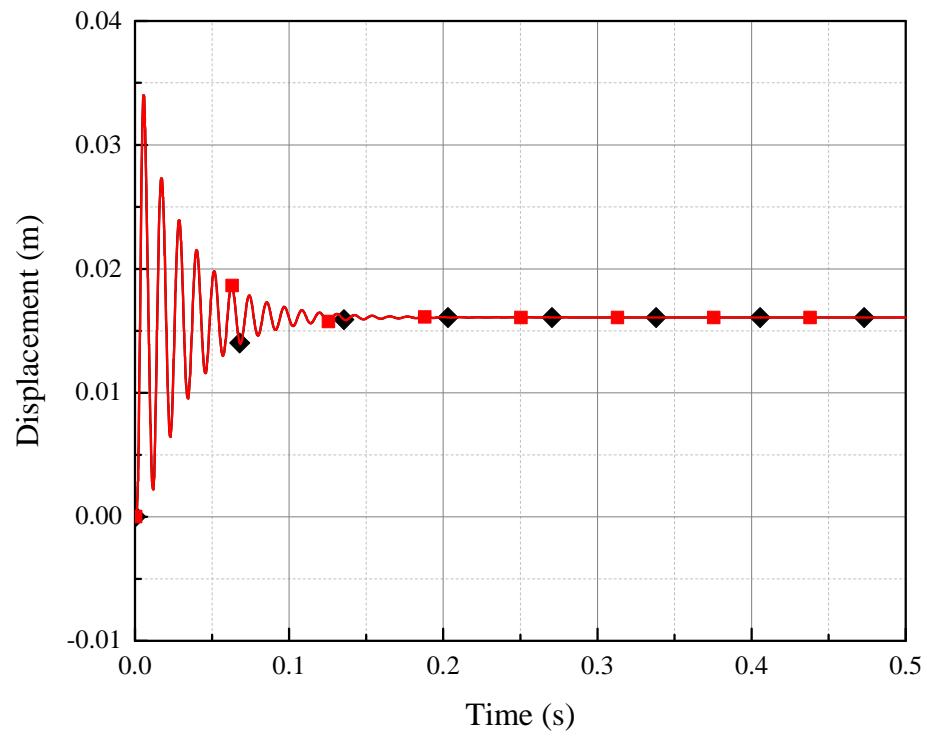
Figure 5 Transverse displacement at the beam free end predicted using FE method
(———◆———Simply-Supported, ———■——— Pinned-Pinned)
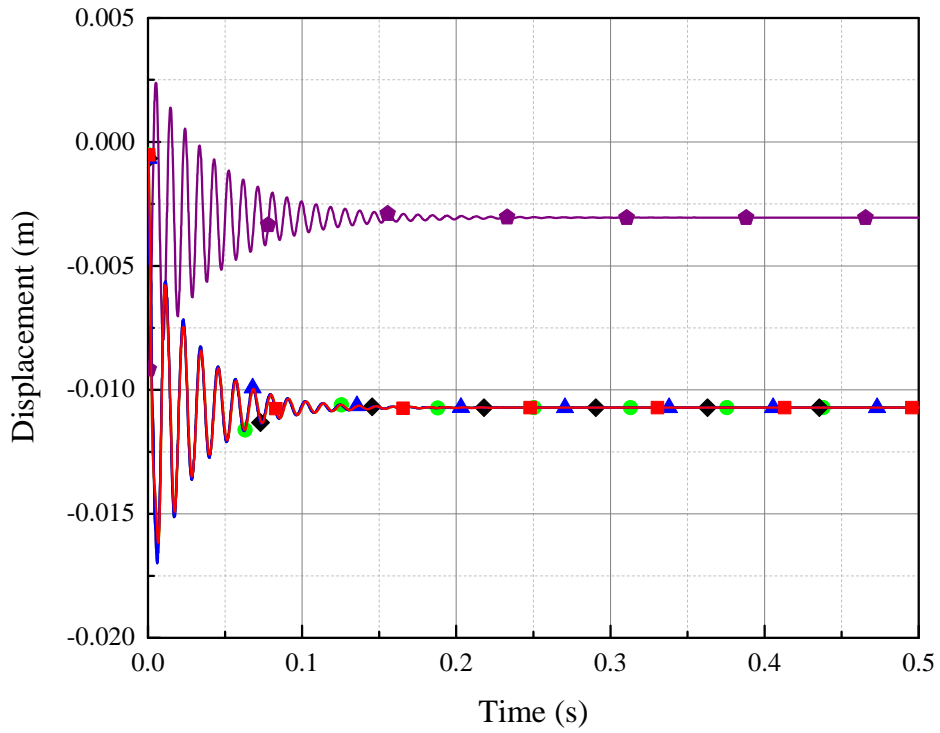
Figure 6 Transverse displacement at the point of the load application predicted using MBS and FE methods

(━━●━━ MBS simply-supported, ━━▲━━ MBS pinned-pinned,

━━◆━━FE simply-supported, ━━■━━ FE pinned-pinned, ━━⬟━━ MBS free-free)
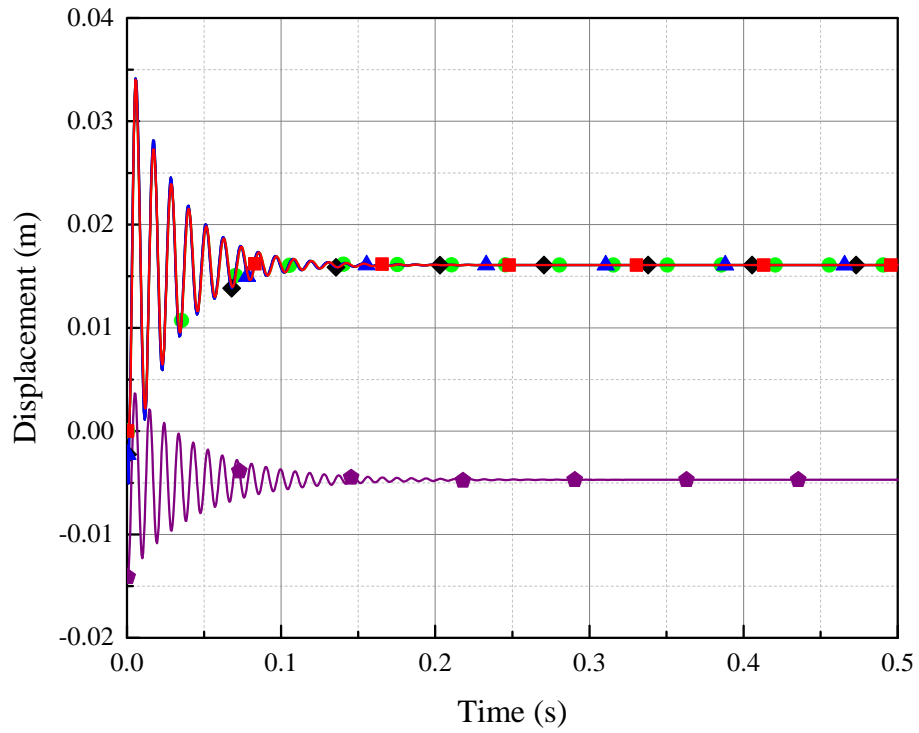
Figure 7 Transverse displacement at the free end predicted using MBS and FE methods
(──●── MBS simply-supported, ──▲── MBS pinned-pinned,
──◆── FE simply-supported, ──■── FE pinned-pinned, ──⬠── MBS free-free)
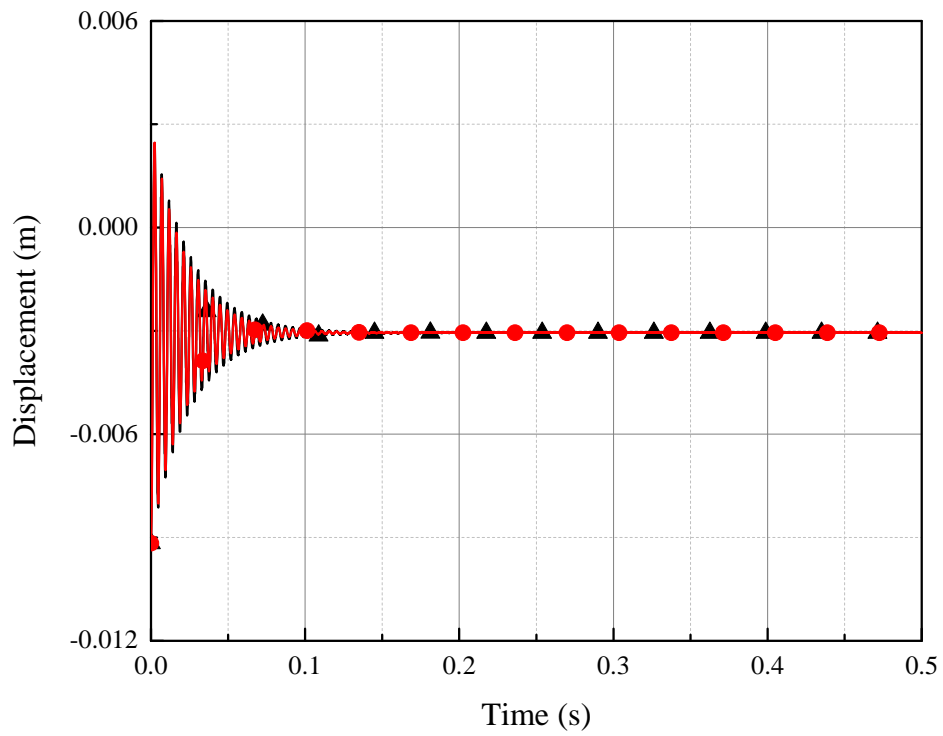
Figure 8 Transverse displacement of the point of the load application in the case of free-free
reference conditions
(——●—— Analytical solution, ——▲—— MBS solution)
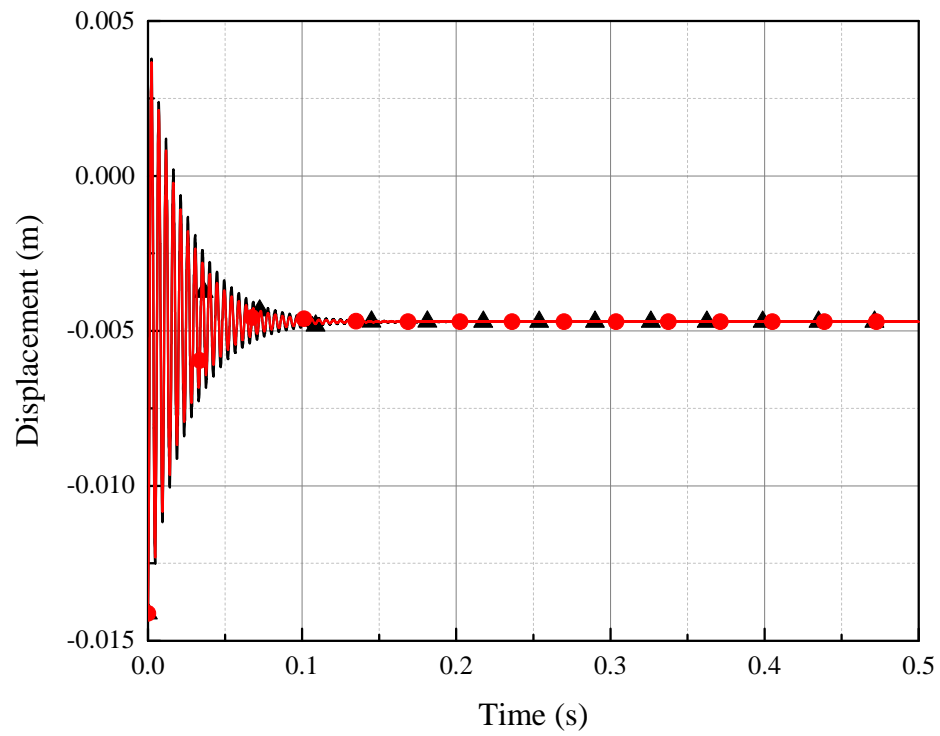
Figure 9 Transverse displacement of the free end in the case of free-free reference conditions
(──●── Analytical solution, ──▲── MBS solution)
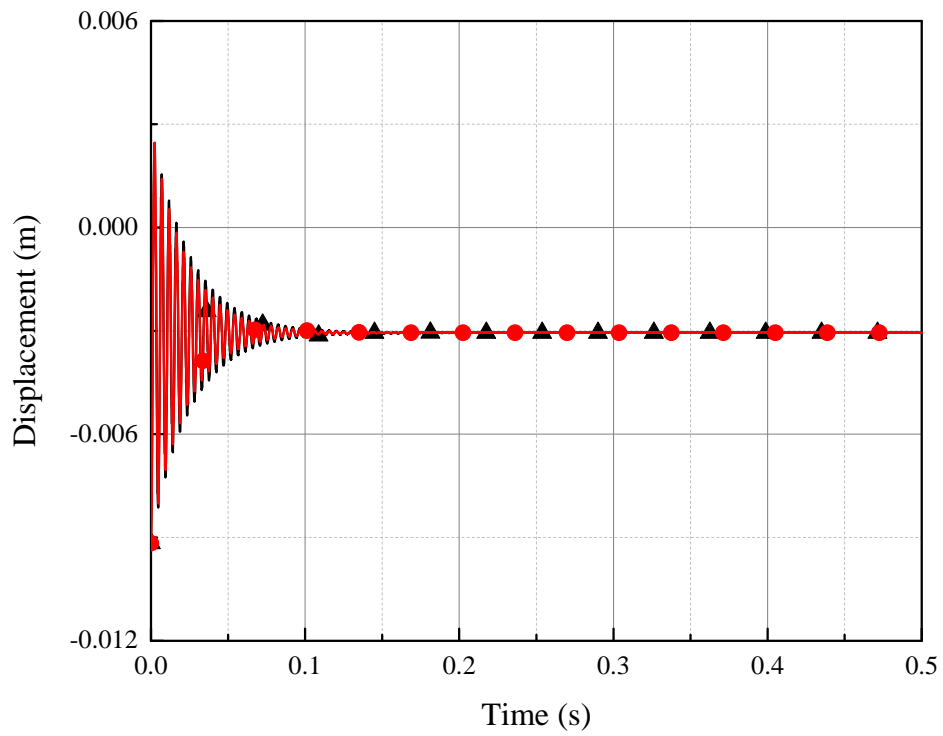
Figure 10 Motion of the body reference in the case of the free-free reference conditions
(———●——— Analytical solution, ———▲———MBS solution)
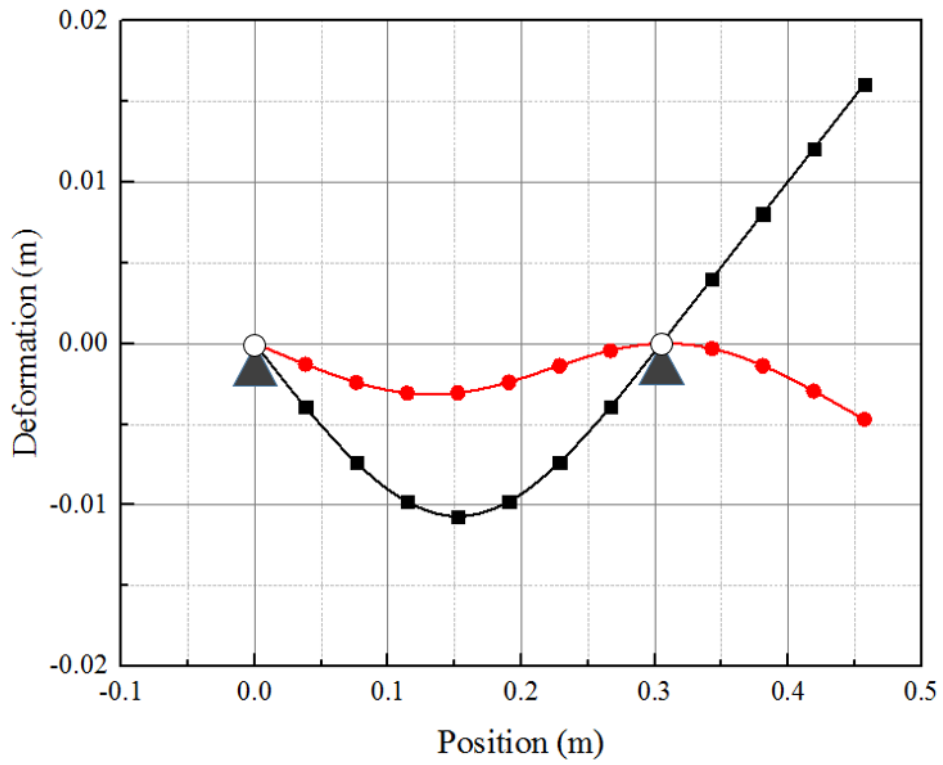
Figure 11 Deformed shape of the beam
(●— Free-Free, ■— Simply-Supported)